Accepted Manuscript

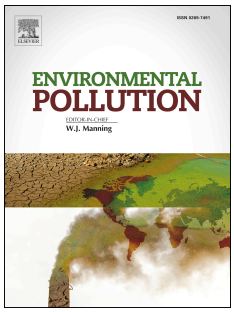

Contributions of local pollution emissions to particle bioreactivity in downwind cities in China during Asian dust periods

Kin-Fai Ho, Kuan-Che Wu, Xinyi Niu, Yunfei Wu, Chong-Shu Zhu, Feng Wu, Jun-Ji Cao, Zhen-Xing Shen, Ta-Chih Hsiao, Kai-Jen Chuang, Hsiao-Chi Chuang

PII: S0269-7491(18)33555-3

DOI: https://doi.org/10.1016/j.envpol.2018.11.035

Reference: ENPO 11862

To appear in: *Environmental Pollution*

Received Date: 2 August 2018

Revised Date: 12 November 2018

Accepted Date: 12 November 2018

Please cite this article as: Ho, K.-F., Wu, K.-C., Niu, X., Wu, Y., Zhu, C.-S., Wu, F., Cao, J.-J., Shen, Z.-X., Hsiao, T.-C., Chuang, K.-J., Chuang, H.-C., Contributions of local pollution emissions to particle bioreactivity in downwind cities in China during Asian dust periods, *Environmental Pollution* (2018), doi: https://doi.org/10.1016/j.envpol.2018.11.035.

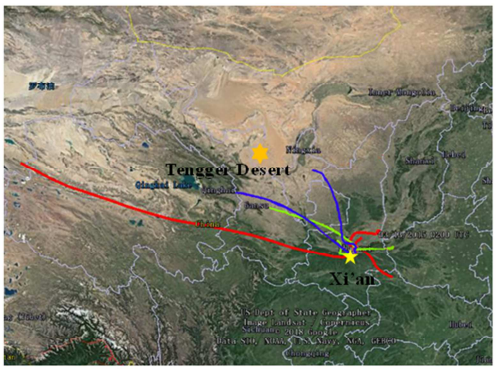

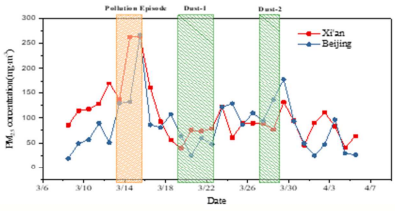

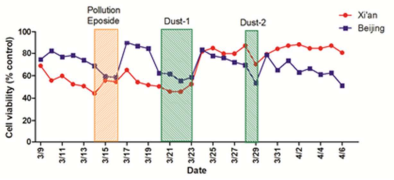

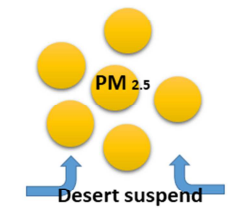

Pollutant carrier

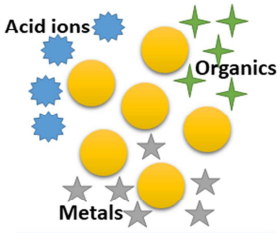

Pollutant interaction

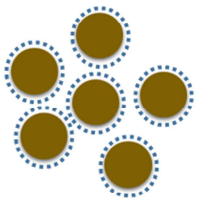

Toxicity increase

Contributions of local pollution emissions to particle bioreactivity in downwind cities in China during Asian dust periods

Kin-Fai Ho[1], Kuan-Che Wu[2], Xinyi Niu[1], Yunfei Wu[3], Chong-Shu Zhu[4,5], Feng Wu[4,5], Jun-Ji Cao[5], Zhen-Xing Shen[6], Ta-Chih Hsiao[7], Kai-Jen Chuang[8,9], Hsiao-Chi Chuang[2,9,10]*

[1]Jockey Club School of Public Health and Primary Care, The Chinese University of Hong Kong, Hong Kong, China

[2]School of Respiratory Therapy, College of Medicine, Taipei Medical University, Taipei, Taiwan[3]CAS Key Laboratory of Regional Climate-Environment for Temperate East Asia, Institute of Atmospheric Physics, Chinese Academy of Sciences, Beijing, China

[4]Key Laboratory of Aerosol Chemistry & Physics, Institute of Earth Environment, Chinese Academy of Sciences, Xi'an, China

[5]SKLLQG, Institute of Earth Environment, Chinese Academy of Sciences, Xi'an, China

[6]Department of Environmental Science and Engineering, Xi'an Jiaotong University, Xi'an, China

[7]Graduate Institute of Environmental Engineering, National Taiwan University, Taipei, Taiwan

[8]Department of Public Health, School of Medicine, College of Medicine, Taipei Medical University, Taipei, Taiwan

[9]School of Public Health, College of Public Health, Taipei Medical University, Taipei, Taiwan

[10]Division of Pulmonary Medicine, Department of Internal Medicine, Shuang Ho Hospital, Taipei Medical University, New Taipei City, Taiwan

Running Head: Local pollution associated with bioreactivity of dust $PM_{2.5}$

Word count: 4,303 [excluding abstract (195 words) and references]; 3 tables; 4 figures.

*** Corresponding Author**

Hsiao-Chi Chuang, PhD

Taiwan CardioPulmonary Research (T-CPR) Group, School of Respiratory Therapy, College of Medicine, Taipei Medical University, Taipei, Taiwan.

Telephone: +886-2-27361661 ext. 3515. Fax: +886-2-27391143. E-mail: r92841005@ntu.edu.tw

Authors' contributions

All authors have contributed substantially to the concept and design of the study, drafting of the article, and critically revising the manuscript for important intellectual content. All authors have read and approved the final version of the manuscript for publication.

Conflict of interest

The authors declare that they have no conflicts of interest.

Fundings

This study was founded by the Ministry of Science and Technology of Taiwan (105-2633-B-038-001 and 106-2633-B-038 -001 for HCC), Research Grants Council of the Hong Kong Special Administrative Region of China (Project No. 14212116 for KFH) and Research Grants Council of the Hong Kong Special Administrative Region (CRF/C5022-14G for KFH).

Acknowledgements

The authors wish to thank Miss Yi-Syuan Lin for the technical assistance of this research.

Supporting Information

The estimation of reconstructed mass concentration is provided in the supplementary information. Table S1 shows the source profile for resuspension dust sample in $PM_{2.5}$ from in Tengger Desert ($\mu g \cdot \mu g^{-1}$). Table S2 shows the correlations of chemical components between different events from Xi'an and Beijing and dust sample from Tengger Desert. Figure S1 shows the source profiles for $PM_{2.5}$ from (a) Xi'an and (b) Beijing. Figure S2 shows thesource profile for resuspension dust sample in $PM_{2.5}$ from in Tengger Desert ($\mu g \cdot \mu g^{-1}$).

Abstract

This study investigated the effects of pollution emissions on the bioreactivity of $PM_{2.5}$ during Asian dust periods. $PM_{2.5}$ during the sampling period were 104.2 and 85.7 $\mu g \cdot m^{-3}$ in Xi'an and Beijing, respectively, whereas $PM_{2.5}$ which originated from the Tengger Desert was collected (dust background). Pollution conditions were classified as non-dust days, pollution episode (PE), dust storm (DS)-1, and DS-2 periods. We observed a significant decrease in cell viability and an increase in LDH that occurred in A549 cells after exposure to $PM_{2.5}$ during a PE and DS-1 in Xi'an and Beijing compared to Tengger Desert $PM_{2.5}$. Positive matrix factorization was used to identify pollution emission sources. $PM_{2.5}$ from biomass and industrial sources contributed to alterations in cell viability and LDH in Xi'an, whereas vehicle emissions contributed to LDH in Beijing. OC, EC, Cl^-, K^+, Mg^{2+}, Ca, Ti, Mn, Fe, Zn, and Pb were correlated with cell viability and LDH for industrial emissions in Xi'an during DS. OC, EC, SO_4^{2-}, S, Ti, Mn, and Fe were correlated with LDH for vehicle emissions in Beijing during DS. In conclusion, the dust may carry pollutants on its surface to downwind areas, leading to increased risks of particle toxicity.

Keywords: air pollution, dust storm, metal, physicochemistry, source apportionment.

Capsule of main finding

The significance and novelty of this study was that sand dust may provide a platform to intermix with chemicals on its surfaces, thereby increasing the bioreactivity of $PM_{2.5}$ during dust storm episodes.

1. Introduction

Asian dust storms, that originate from deserts of northern/northwestern China, often move to surrounding areas during late winter and spring (Lee et al., 2003). Dust storm events often occur in upwind regions in spring, such as from the Tengger Desert. Even after being transported thousands of miles, dust is able to decrease visibility and, more importantly, deteriorate the air quality of downwind areas (Chan et al., 2008; Chan and Ng, 2011; Lee et al., 2006). Epidemiological evidence reported that pulmonary exposure to particulate matter of <2.5 μm in aerodynamic diameter ($PM_{2.5}$) increased the risk of hospital admissions, cardiovascular disease, and pulmonary disease during dust storm episodes (Chan et al., 2008; Chan and Ng, 2011; Ma et al., 2017; Teng et al., 2016). Although numerous reports indicated associations between adverse human health impacts and dust storm exposure, causal relationships are still not very clear. In contrast, there are still many studies that observed insignificant effects of dust storms on human health outcomes, even though the particulate matter of <10 μm in aerodynamic diameter (PM_{10}) mass concentrations were significantly higher on dust storm days than non-dust storm days (Chen et al., 2004; Lee et al., 2007). This may have been due to the complexity of the physicochemical characteristics of $PM_{2.5}$ during dust storm events.

Environmental impacts and health risks associated with Asian dust storms are of great concern to downwind regions. For example, the long-range transport of bacteria and viruses by dust storm was previously reported (Chen et al., 2010; Garrison et al., 2003). Cardiopulmonary effects caused by long-range transport of dust storm have also been identified in numerous down-wind regions, where the risk of stroke (Kang et al., 2013), ischemic heart diseases, cerebrovascular diseases, chronic obstructive pulmonary diseases (Chan et al., 2008; Crooks et al., 2016; Tam et al., 2012), asthma (Watanabe et al., 2011) were increased during the dust storm episodes. Generally, dust sand has relative lower particle toxicity than urban dust based on the same mass concentration. However, dust sand could act as a "carrier" to interact with pollutants during transportation in the atmosphere. The dust sand could play the role of "Trojan horse" that provides a platform to interact with chemicals on its surface. Therefore, the particles toxicity or health outcomes on the downwind receptor regions may be distinct difference due to its final physicochemical characteristics.

The Tengger Desert is the fourth largest desert in China, and is an important source of dust storms (Wang et al., 2005; Zhang et al., 2008). Desert dust suspended in the atmosphere and carried to northern and eastern regions is one of the important pathways of dust storm transport (Sun et al., 2001). Notably, the rapid industrialization of China has produced large amounts of pollutants that can interact with dust storm particles, thereby adding to concerns regarding health impacts of pulmonary exposure to dust

storms which require human health protection. However, contributions of local pollutions to $PM_{2.5}$ bioreactivity during dust storm events remain unclear. The objective of this study was to investigate the effects of local pollution emissions on $PM_{2.5}$ bioreactivity during dust periods. Emission sources of $PM_{2.5}$ in two downwind cities (Xi'an and Beijing) were determined during dust periods, and we examined contributions of the $PM_{2.5}$ emission sources and chemical constituents of the $PM_{2.5}$ to its bioreactivity *in vitro*.

2. Materials and Methods

2.1. Particle collection

$PM_{2.5}$ samples were collected in Xi'an and Beijing during dust periods weather from 9 March to 7 April 2015. Xi'an, located in Northwest China, is the capital city of Shaanxi Province with industries in or around the city. Beijing, located in the North of North China Plain, is the economy and politics central of China, while industries were all moved away from the city. Xi'an and Beijing both show the continental monsoon climate, and spring is always dry, windy and changeable. The sampling site in Xi'an has been reported previously (Shen et al., 2010). Briefly, $PM_{2.5}$ was collected from the campus of Xi'an Jiaotong University, where was between major roads with heavy traffic and residential areas. The sampling site in Beijing was carried out at the Tower Division of the Institute of Atmospheric Physics, Chinese Academy of Sciences, where was surrounded by residential areas located near a busy highway.

$PM_{2.5}$ samples were collected every day from 10:00 to 10:00 (24 hrs) during the sampling period. Parallel sampling of $PM_{2.5}$ was collected on quartz filters (Whatman, UK) for chemical analyses and collected on Teflon filters (Whatman) for the bioreactivity by mini-volume air samplers (Airmetrics, Eugene, OR, USA) with a flow rate of 5 $L \cdot min^{-1}$. Quartz filters were pre-heated before sampling to 600 °C for 3 h, and all filters were conditioned at 20~23 °C and 35%~45% relative humidity (RH) for equilibration. Mass of the filters were obtained using an electronic microbalance (MC5, Sartorius, Göttingen, Germany). More details on the $PM_{2.5}$ mass analysis and quality control were described by Cao *et al.*(2012).

Dust of the Tengger Desert was analyzed for a dust source profile, and was collected from representative portions of the desert surface 99 km away from national highway S218 (40°0'56"N; 104°55'35"E). The collected dust samples were stored in labeled polyethylene bags followed by air-dried at about 25 °C for 1 week to remove moisture. Samples were sieved through Tyler sieves of 30, 50, 100, 200, and 400 mesh to obtain ~5 g of particles (with diameters of < 38 μm). The sieved samlpe was then re-suspended in a chamber and sampled through $PM_{2.5}$-selective inlets onto 47-mm quartz filters for chemical analyses,

whereas samples were collected onto Teflon filters for bioreactivity (Chow et al., 1994; Wu et al., 2011b).

2.2. Chemical characterization

Anions (Cl^-, NO_3^-, and SO_4^{2-}) and cations (NH_4^+, K^+, Mg^{2+}, and Ca^{2+}) were determined in aqueous extracts of sample filters as reported previously (Shen et al., 2009). Briefly, a Dionex-600 Ion Chromatograph (Dionex, Sunnyvale, CA, USA) was used for the cation and anion analyses, with an IonPacCS12A column and IonPac AS14A column, respectively (Zhang et al., 2011). A DRI model 2001 carbon analyzer (Atmoslytic, Calabasas, CA, USA) was used to determine the levels of organic carbon (OC) and elemental carbon (EC) according to the IMPROVE thermal/optical reflectance (TOR) protocol (Cao et al., 2007). OC fractions (OC1, OC2, OC3, and OC4), OP (a pyrolyzed carbon fraction), and EC fractions (EC1, EC2, and EC3) were determined according to our previous report (Cao et al., 2012). OC was defined as OC1 + OC2 + OC3 + OC4 + OP. EC was defined as EC1 + EC2 + EC3 – OP.

S, Ca, Ti, V, Mn, Fe, Zn, and Pb in $PM_{2.5}$ were determined using an Energy-dispersive x-ray fluorescence (ED-XRF) spectrometry (PANalytical Epsilon 5, Almelo, Netherlands). The ED-XRF spectrometer was calibrated with thin-film standards obtained from MicroMatter (Arlington, WA, USA) (Xu et al., 2012). Data were corrected for field blanks, and duplicated samples were analyzed for error assurance.

2.3. Source apportionment

Positive matrix factorization (PMF) was applied to identify presumptive sources of the $PM_{2.5}$ collected in Xi'an and Beijing. PMF developed by Paatero and colleagues has been widely used for source-apportionment receptor modeling (Paatero, 1997; Paatero and Tapper, 1994), which has no limitations on source numbers and does not require source profile information (Wang et al., 2015). In this study, the mass concentration, two carbons, five ions, and 12 elements were included in the model EPA PMF 5.0: OC, EC, Cl^-, SO_4^{2-}, NO_3^-, NH_4^+, K^+, Ca, Mg, Ti, Mn, Cr, Co, Fe, Ni, Cu, Zn, Pb, and Ba. Concentrations and equation-based uncertainties of chemical species were input into the model, of which uncertainty included detection limits and error fractions (10%). The PMF model was run multiple times, each run was initialized with random starting points. The most physically interpretable profiles were found with a six-factor solution.

2.4. Particle preparation

$PM_{2.5}$ was removed from the filters using two-stage sonication in methanol according to our previous report (Chuang et al., 2013). Samples were then dried with a nitrogen stream. A $PM_{2.5}$ stock solution (1

mg/mL) was prepared in < 0.01% vol dimethyl sulfoxide (DMSO) in phosphate-buffered saline (PBS). Fresh samples were kept at 4 °C and used within 1 week of preparation.

2.5. Cell culture and treatment

Human A549 alveolar epithelial cells (American Type Culture Collection; Manassas, VA, USA) were cultured in RPMI medium (10% fetal bovine serum, penicillin, and streptomycin) at 37 °C with 95% humidity and 5% CO_2. Cells (10^5 cells/mL). Cells were exposed to 0 and 50 μg/mL of $PM_{2.5}$ in serum-free RPMI medium for 16 hrs. After exposure, cells were analyzed for cell viability, whereas the supernatants were analyzed for lactate dehydrogenase (LDH).

2.6. Cell viability

A sulforhodamine B (SRB) colorimetric assay was used to examine cell viability according to a previous method (Vichai and Kirtikara, 2006). Briefly, cells were fixed and stained with 10% (wt/vol) trichloroacetic acid. A 10 mM Tris base solution was used to dissolve the protein-bound dye. A microplate reader was used to determine the OD at 510 nm. Cell viability (%) was presented after adjusting for the control.

2.7. LDH

An enzyme-linked immunosorbent assay (ELISA) was used in the LDH Cytotoxicity Assay Kit (Thermo Scientific, Waltham, MA, USA) according to the manufacturer's instructions.

2.8. Statistical analysis

Data are expressed as the mean ± standard deviation (SD). One-way analysis of variance (ANOVA) with Tukey's *post-hoc* test was used to compare multiple values. Residual values were evaluated for independence by means of the Durbin–Watson test. Pearson's correlation coefficient was used to examine the correlation of $PM_{2.5}$ (mass concentration and chemicals) and its bioreactivity. Statistical analyses were performed using GraphPad vers. 5 for Windows. Durbin–Watson test was performed using SPSS vers. 20 for Windows. The level of significance was set to $p<0.05$. All experiments were performed in quintuplicate.

3. Results and Discussion

3.1. Characterization of $PM_{2.5}$

Average $PM_{2.5}$ concentrations during the study period were 104.2 and 85.7 $\mu g \cdot m^{-3}$ in Xi'an and Beijing, respectively. Daily $PM_{2.5}$ concentrations in the two cities are shown in Figure 1. It was found that the $PM_{2.5}$ pollution level in Xi'an was consistently higher than that in Beijing in the sampling period. In order to determine particle transport from nearby deserts to Xi'an and Beijing, back trajectories for the cities on pollution days are shown in Figure 2. Different pollution conditions were classified as normal

days, pollution episodes (PEs), dust storm periods (DS)-1, and DS-2. On 26~28 March (PE), Xi'an and Beijing suffered from heavy pollution with $PM_{2.5}$ concentrations of as high as 221.1 and 175.9 $\mu g \cdot m^{-3}$, both of the cities were mainly influenced by anthropogenic emissions with low diffusion conditions, and Beijing was affected by the transportation of pollutants from nearby heavy-industry cities. The $PM_{2.5}$ peaks on 20~23 (DS-1) and 28~29 March (DS-2) were mainly caused by a dust storm. In Xi'an, fugitive dust from construction sites and suburban areas were the main sources during DS-1. While during DS-2, the high level of pollution was dominated by dust transported from the Tengger Desert, which is 800 km away from Xi'an city. During the sampling period, DS-1 was mainly influenced by a dust storm from the Otindag Sandy Land, which was only 180 km away from Beijing City. Pollution in DS-2 was caused by transport from The Kirchten Desert about 600 km away from Beijing and also regional fugitive dust emissions. The land-surface usage between these deserts and Xi'an and Beijing mostly are agriculture areas in northern China. There are also some populated areas between the desert and the cities where anthropogenic emissions were usually observed due to human activities (Wu et al., 2017).

3.2. Chemical characterization of $PM_{2.5}$

$PM_{2.5}$ concentrations and chemical compositions that contributed to $PM_{2.5}$ in Xi'an and Beijing are shown in Table 1. 73.0~91.8% of $PM_{2.5}$ mass was reconstructed by Equation S1 in supplementary material. On normal days, the OC concentration in Beijing (12.8 $\mu g \cdot m^{-3}$) was higher than that in Xi'an (11.7 $\mu g \cdot m^{-3}$), while the EC concentration in Xi'an (4.4 $\mu g \cdot m^{-3}$) was higher than that in Beijing (3.6 $\mu g \cdot m^{-3}$). It was found that OC contributed more to $PM_{2.5}$ in Beijing, and the OC/EC ratio in Beijing (3.8) was higher than that in Xi'an (2.8), which indicated that more-frequent combustion emissions would lead to the transformation of secondary OC (SOC). NO_3^-, SO_4^{2-}, and NH_4^+ were major ions in $PM_{2.5}$, and collectively contributed 45.7% and 37.8% to total $PM_{2.5}$ in Xi'an and Beijing, respectively, on normal days. Concentrations and contributions of these secondary ions in Xi'an were much higher than in Beijing, and this was mainly caused by local emissions of combustion products (such as industrial emissions) with photo-oxidation. It was also found that the contribution of NO_3^- obviously increased on pollution days due to combustion activities, while in DS periods, NO_3^- and NH_4^+ contributions to $PM_{2.5}$ showed an obvious decreasing trend. As an indicator of mineral dust (Zhang et al., 2011), Ca^{2+} showed higher contribution in Beijing than in Xi'an, which indicated that fugitive dust from deserts contributed more to $PM_{2.5}$ in Beijing. During DS-1 in Beijing, the contribution of Ca^{2+} was as high as 11.3%, indicating a major contribution of fugitive dust instead of anthropogenic emissions during the dust periods.

S showed higher contributions in Xi'an (3.3%) than in Beijing (2.0%) on normal days, and showed the highest concentration among the detected elements, which was mainly contributed by anthropogenic activities in the local region. As an indicator of crustal origin, Ca and Fe respectively contributed 0.4% and 0.5% in Xi'an and 2.7% and 1.2% in Beijing on normal days. During DS-1, the concentration of Ca was highly correlated with Fe (R^2=0.95) in Beijing, while Ca^{2+} showed a low correlation with Fe (R^2=0.26), indicating a high contribution of dust storm sources with elemental Ca. Respective Fe/Ca ratios in Xi'an and Beijing were 2.27 and 0.49 on normal days. During DS periods, the Fe/Ca ratios showed lower levels in Xi'an, which were 0.84 and 1.01 during DS-1 and DS-2, respectively; while in Beijing, Fe/Ca ratios increased to 0.61 (DS-1) and 1.14 (DS-2). Compared to Fe/Ca results in desert soil in China of 0.57 (Ta et al., 2003), the $PM_{2.5}$ on dust transport days, especially in Beijing (DS-1), was similar to characteristics of Asian dust (Cao et al., 2008). Beijing was more affected by the transport of dust from the nearby desert in Inner Mongolia, which resulted in higher contributions of dust to $PM_{2.5}$.

The source profile for dust from $PM_{2.5}$ in the Tengger Desert is shown in Table S1. Ca and Fe were the most abundant constituents in the dust sample, among which, Ca showed the highest contribution of 6.2% followed by Fe (3.9%). Abundant crucial materials were indicated by OC, which contributed 2.7% to the dust sample. The relatively high concentration of OC was mainly from carbonate carbon, which is also one of the main constituents of dust. EC was not detected in the sample due to the location being far away from highways and residential areas. As to anthropogenic sources of these components, they always showed low concentrations in dust, of which NO_3^- and SO_4^{2-} only contributed 0.3%, while Zn, Pb, Ni, Cu, and Hg were in the range of 0.004%~0.015%. Comparing with dust profiles from other deserts (i.e. Chinese Loess Plateau, Taklimakan Desert, Xinjiang Gobi, et al.), the dust showed the similar patterns that organic carbon, Ca and Fe are the major contributors, and contributions of other elements differed from each other slightly (Wu et al., 2011a; Zhang et al., 2014). The correlations of the chemical components between different events and the dust sample was shown in Table S2. The environmental $PM_{2.5}$ did not shown good correlations with the desert sample due to the complex emissions and reactions in the atmosphere. While in Beijing DS-1 the $PM_{2.5}$ showed moderate correlation with the dust sample, indicated the contribution of dust from nearby desert to Beijing.

3.3. Source apportionment

PMF was applied to identify the sources and relative contributions of each source to $PM_{2.5}$ during the study period in both Xi'an and Beijing. Results of the source apportionment for the two cities and daily contributions of each source are shown in Figure 3, and the identified source profiles are shown in Figure S1. Coal combustion (37.2%) was the dominant contributor to $PM_{2.5}$ in Xi'an, while secondary

inorganic aerosols (SNAs) (31.5%) showed the highest contribution in Beijing. In addition, vehicle emissions were the second-highest contributor to $PM_{2.5}$ in both cities, accounting for 21.3% in Xi'an and 19.7% in Beijing. It was found that the greatest contributions to $PM_{2.5}$ were mostly by fossil fuel combustion and secondary products (i.e., the sum of SNAs, vehicles, coal, and biomass) which accounted for 85.4% in Xi'an and 68.7% in Beijing. Whereas Xi'an suffered more from primary pollution, Beijing was more polluted by secondary aerosols. Dust had a high contribution (18.2%) in Beijing, which was due to being more closely located to the desert area and the transportation route. Source profiles in this study were consistent with previous studies (Wang et al., 2015; Zhang et al., 2013), and compared to previous results, the contribution of dust in spring was higher than in other seasons in both Xi'an and Beijing. Daily variations in source contributions showed that during DS-1 and DS-2, dust emissions accounted for 20%~30% in Xi'an and over 40% in Beijing, indicating the transport of dust during pollution episodes.

3.4. Bioreactivity of $PM_{2.5}$

To investigate the bioreactivity caused by $PM_{2.5}$ collected in Xi'an and Beijing during the study period, cell viability and LDH (an indicator of cytotoxicity) were determined in A549 cells. Daily variabilities in cell viability and LDH after $PM_{2.5}$ exposure are shown in Figure 4. $PM_{2.5}$ collected from the Tengger Desert served as a dust control. Tengger Desert $PM_{2.5}$ was pure control particles with no interactions with pollution during transport. We observed that cell viability more significantly (p<0.05) decreased after exposure to $PM_{2.5}$ during a PE and DS-1 in Xi'an and Beijing than after exposure to Tengger Desert $PM_{2.5}$. Similarly, LDH significantly (p<0.05) increased after exposure to $PM_{2.5}$ during a PE and DS-1 in Xi'an and Beijing than after exposure to Tengger Desert $PM_{2.5}$. Notably, there was distinct difference of the $PM_{2.5}$ bioreactivity between the two DS events. We observed that $PM_{2.5}$ from DS-1 caused alteration in cell viability and LDH in Xi'an and Beijing. But $PM_{2.5}$ collected from Beijing caused significant alteration than $PM_{2.5}$ collected from Xi'an during DS-2. Together, the results suggested that the $PM_{2.5}$ mixture and/or chemical reconstruction could have occurred in the atmosphere during transport from the desert. Next, we observed that the cell viability significantly (p<0.05) decreased after $PM_{2.5}$ exposure during a PE and DS-1 compared to normal days in Xi'an, whereas cell viability significantly (p<0.05) decreased after $PM_{2.5}$ exposure during DS-1 compared to normal days in Beijing. Also, cell viability was significantly (p<0.05) reduced by $PM_{2.5}$ during DS-1 compared to DS-2 in Xi'an. As to cytotoxicity, we observed that $PM_{2.5}$ caused significant (p<0.05) increases in LDH compared to normal days in both Xi'an and Beijing. LDH significantly (p<0.05) increased after $PM_{2.5}$ exposure during DS-1 compared to DS-2 in Xi'an. Consistently, a previous report showed that PM

collected from dust storms induced decreases in cell viability and LDH production (Naimabadi et al., 2016), inflammatory responses (Lei et al., 2004; Watanabe et al., 2015), and DNA damage (Meng and Zhang, 2007). Notably, Watanabe and colleagues (2015) observed that PM collected from different dust storm periods in Japan had different *in vitro* inflammatory potentials (Watanabe et al., 2015). If desert dust has a lower bioreactive potential before transport, the pollutant interactions or chemical absorption onto particle surfaces could modify the particle bioreactivity. Therefore, local pollution emission sources could have distinct effects upon $PM_{2.5}$ bioreactivity during DS periods.

3.5. $PM_{2.5}$ bioreactivity and emission sources

The bioreactivity of $PM_{2.5}$ showed significant differences between a desert origin and a PE or DS. However, results could not represent contributions of local pollution emissions to the bioreactivity by $PM_{2.5}$ in downwind areas. To understand the effects of $PM_{2.5}$ emitted from different emission sources (based on source apportionment), we correlated the bioreactivity to $PM_{2.5}$ levels with the emission sources. First, we found that $PM_{2.5}$ was negatively correlated with cell viability during normal days in Xi'an, whereas $PM_{2.5}$ was positively correlated with LDH during dusty days (DS-1 and DS-2) in Beijing (Table 2). To understand the contribution of $PM_{2.5}$ bioreactivity during the entire study period (all), normal days (normal), and dust storms (dust), $PM_{2.5}$ levels emitted from six sources (i.e., biomass, coal, industry, vehicles, SNAs, and dust) were correlated with $PM_{2.5}$ bioreactivity (cell viability and LDH) (Table 2). We observed that cell viability and LDH were significantly associated with $PM_{2.5}$ levels from industrial and vehicle emissions during the entire study period in Xi'an, and associations of cell viability and LDH with industrial and vehicle were also observed on normal days. Notably, cell viability and LDH were correlated with $PM_{2.5}$ from biomass and industry during dust storms in Xi'an. As to results from Beijing, we observed that vehicles were associated with cell viability and LDH on normal days and LDH during dust storms. Sand dust from the desert is of geological origin, which commonly consists of silicon dioxide, aluminum oxide, iron (III) oxide, calcium oxide, magnesium oxide, etc. (Zaady et al., 2001). Although a previous report indicated that sand dust is able to induce inflammation (Zosky et al., 2014), more evidence showed that organic fractions of $PM_{2.5}$ collected during dust storm episodes contributed to cell viability, LDH, and DNA damage (Meng and Zhang, 2007; Naimabadi et al., 2016). Notably, in the present study, desert dust was not significantly associated with cell viability or LDH in Xi'an or Beijing during the study periods. This may have resulted from higher contributions of local pollutants than the dust itself. In the present study, $PM_{2.5}$ produced by local emission sources (such as biomass and industry in Xi'an and vehicles in Beijing) may have contributed to the deterioration in local pollutant emissions during dust storm periods, leading to increased particle bioreactivity.

3.6. $PM_{2.5}$ bioreactivity and chemical components

Chemical constituents are recognized as critical determinants regulating particle toxicity (Lee et al., 2014; Lui et al., 2016). The chemical profile of $PM_{2.5}$ is known to be associated with emission sources (Chuang et al., 2018); therefore, it is important to classify contributions of chemical fractions of $PM_{2.5}$ to its bioreactivity by different emission sources. Based on our previous report, we successfully identified chemical contributions of $PM_{2.5}$ by emission sources (source apportionment) to particle bioreactivity (*in vitro* results) (Chuang et al., 2018). Because of the data was obtained daily during the study period, we first examined the independence of the variables (bioreactivity and $PM_{2.5}$) with time using Durbin-Watson test. The Durbin-Watson values were 0.816 for LDH and 0.735 for cell viability in Xi'an, whereas the values were 1.731 for LDH and 1.481 for cell viability in Beijing. Therefore, Pearson's correlation coefficients were further used to examine correlations between chemical compounds of associated $PM_{2.5}$ sources (biomass and industry in Xi'an and vehicles in Beijing) and bioreactivity (cell viability and LDH) during the entire study period (all) and during dust storms (dust) (Table 3). We observed that Ca^{2+} and Zn were associated with cell viability, and OC and Ca^{2+} were associated with LDH for biomass emissions in Xi'an during the entire study period. Most of the chemical components measured in this study were correlated with cell viability (except for Ca^{2+}, Ca, and Ti) and LDH (except for Zn) in Xi'an for industrial emissions during the entire study period. But no correlations were identified between vehicle-emitted chemicals and cell viability or LDH during the entire study period. We further explored the contributions of chemicals by emission sources to bioreactivity during dust storms. Notably, Cl^-, NO^{3-}, and Ca were associated with cell viability and LDH for biomass emissions in Xi'an during dust storms. OC, EC, Cl^-, K^+, Mg^{2+}, Ca, Ti, Mn, Fe, Zn, and Pb were correlated with cell viability and LDH for industrial emissions in Xi'an during dust storms. We only observed that OC, EC, SO_4^{2-}, S, Ti, Mn, and Fe were correlated with LDH for vehicle emissions in Beijing during dust storms. The observations suggest that more-detailed associations between chemicals of $PM_{2.5}$ and bioreactivity could be obtained based on further analyses by source apportionment. Our results showed that OC, EC, acidic ions (i.e., Cl^-, NO^{3-}, and SO_4^{2-}), and metals (i.e., Ti, Mn, Fe, Zn, and Pb) may contribute to increases in $PM_{2.5}$ bioreactivity during dust storm episodes. Our results are in line with previous findings, for which organic fractions, acid ions, and metals were associated with particle bioreactivity (M. et al., 2006; Meng and Zhang, 2007; Naimabadi et al., 2016). If we compare the dust storm with desert $PM_{2.5}$, desert and dust storm $PM_{2.5}$ samples represent distinct chemical profiles. Metals, cations, and anions are transported by particles in the atmosphere, which was reported to cause adverse health effects (Alessandria et al., 2014; Ghio et al., 2012). Inhalation of Cl^-, NO^{3-}, and SO_4^{2-} may change the lung

environment, leading to a pH imbalance. Therefore, it is reasonable to hypothesize that $PM_{2.5}$ bioreactivity during dust storm episodes depends on local pollution emissions or pollution during transportation. On the other hand, desert dust plays a role as a pollutant carrier, which provides a platform to intermix with chemicals on its surface.

4. Conclusions

In conclusion, this is the first study to investigate contributions of emission sources to $PM_{2.5}$ bioreactivity during dust storm periods. Emissions of $PM_{2.5}$ from local pollutant sources could cause deterioration of air quality during dust storms as well increasing particle bioreactivity. Significant amounts of suspended sand dust may provide a platform to intermix with chemicals on its surfaces, thereby increasing the bioreactivity of $PM_{2.5}$ during dust storm episodes. Dust may carry pollutants on its surface to downwind areas, leading to increased risks of cardiopulmonary diseases. Our findings suggest that reducing local pollutant emission sources may be important for reducing potential health impacts during Asian dust storms.

References

Alessandria, L., Schiliro, T., Degan, R., Traversi, D., Gilli, G., 2014. Cytotoxic response in human lung epithelial cells and ion characteristics of urban-air particles from Torino, a northern Italian city. Environ Sci Pollut Res Int 21, 5554-5564.

Cao, J.J., Chow, J.C., Watson, J.G., Wu, F., Han, Y.M., Jin, Z.D., Shen, Z.X., An, Z.S., 2008. Size-differentiated source profiles for fugitive dust in the Chinese Loess Plateau. Atmospheric Environment 42, 2261-2275.

Cao, J.J., Lee, S.C., Chow, J.C., Watson, J.G., Ho, K.F., Zhang, R.J., Jin, Z.D., Shen, Z.X., Chen, G.C., Kang, Y.M., Zou, S.C., Zhang, L.Z., Qi, S.H., Dai, M.H., Cheng, Y., Hu, K., 2007. Spatial and seasonal distributions of carbonaceous aerosols over China. Journal of Geophysical Research-Atmospheres 112, 9.

Cao, J.J., Shen, Z.X., Chow, J.C., Watson, J.G., Lee, S.C., Tie, X.X., Ho, K.F., Wang, G.H., Han, Y.M., 2012. Winter and Summer PM2.5 Chemical Compositions in Fourteen Chinese Cities. Journal of the Air & Waste Management Association 62, 1214-1226.

Chan, C.C., Chuang, K.J., Chen, W.J., Chang, W.T., Lee, C.T., Peng, C.M., 2008. Increasing cardiopulmonary emergency visits by long-range transported Asian dust storms in Taiwan. Environ Res 106, 393-400.

Chan, C.C., Ng, H.C., 2011. A case-crossover analysis of Asian dust storms and mortality in the downwind areas using 14-year data in Taipei. Sci Total Environ 410-411, 47-52.

Chen, P.S., Tsai, F.T., Lin, C.K., Yang, C.Y., Chan, C.C., Young, C.Y., Lee, C.H., 2010. Ambient influenza and avian influenza virus during dust storm days and background days. Environ Health Perspect 118, 1211-1216.

Chen, Y.S., Sheen, P.C., Chen, E.R., Liu, Y.K., Wu, T.N., Yang, C.Y., 2004. Effects of Asian dust storm events on daily mortality in Taipei, Taiwan. Environ Res 95, 151-155.

Chow, J.C., Watson, J.G., Houck, J.E., Pritchett, L.C., Rogers, C.F., Frazier, C.A., Egami, R.T., Ball, B.M., 1994. A laboratory resuspension chamber to measure fugitive dust size distributions and chemical-compositions. Atmospheric Environment 28, 3463-3481.

Chuang, H.C., Cheng, Y.L., Lei, Y.C., Chang, H.H., Cheng, T.J., 2013. Protective effects of pulmonary epithelial lining fluid on oxidative stress and DNA single-strand breaks caused by ultrafine carbon black, ferrous sulphate and organic extract of diesel exhaust particles. Toxicol Appl Pharmacol 266, 329-334.

Chuang, H.C., Shie, R.H., Chio, C.P., Yuan, T.H., Lee, J.H., Chan, C.C., 2018. Cluster analysis of fine particulate matter (PM2.5) emissions and its bioreactivity in the vicinity of a petrochemical complex. Environ Pollut 236, 591-597.

Crooks, J.L., Cascio, W.E., Percy, M.S., Reyes, J., Neas, L.M., Hilborn, E.D., 2016. The Association between Dust Storms and Daily Non-Accidental Mortality in the United States, 1993-2005. Environ Health Perspect 124, 1735-1743.

Garrison, V.H., Shinn, E.A., Foreman, W.T., Griffin, D.W., Holmes, C.W., Kellogg, C.A., Majewski, M.S., Richardson, L.L., Ritchie, K.B., Smith, G.W., 2003. African and Asian Dust: From Desert Soils to Coral Reefs. BioScience 53, 469-480.

Ghio, A.J., Carraway, M.S., Madden, M.C., 2012. Composition of air pollution particles and oxidative stress in cells, tissues, and living systems. J Toxicol Environ Health B Crit Rev 15, 1-21.

Kang, J.H., Liu, T.C., Keller, J., Lin, H.C., 2013. Asian dust storm events are associated with an acute increase in stroke hospitalisation. J Epidemiol Community Health 67, 125-131.

Lee, C.-T., Chuang, M.-T., Chan, C.-C., Cheng, T.-J., Huang, S.-L., 2006. Aerosol characteristics from the Taiwan aerosol supersite in the Asian yellow-dust periods of 2002. Atmos Environ 40, 3409-3418.

Lee, H.N., Tanaka, T., Chiba, M., Igarashi, Y., 2003. Long Range Transport of Asian Dust from Dust Storms and its Impact on Japan. Water, Air and Soil Pollution: Focus 3, 231-243.

Lee, J.T., Son, J.Y., Cho, Y.S., 2007. A comparison of mortality related to urban air particles between periods with Asian dust days and without Asian dust days in Seoul, Korea, 2000-2004. Environ Res 105, 409-413.

Lee, K.-Y., Wong, C.K.-C., Chuang, K.-J., Bien, M.-Y., Cao, J.-J., Han, Y.-M., Tian, L., Chang, C.-C., Feng, P.-H., Ho, K.-F., Chuang, H.-C., 2014. Methionine oxidation in albumin by haze fine particulate matter: an in vitro and in vivo study. J Hazard Mater 274, 384-391.

Lei, Y.C., Chan, C.C., Wang, P.Y., Lee, C.T., Cheng, T.J., 2004. Effects of Asian dust event particles on inflammation markers in peripheral blood and bronchoalveolar lavage in pulmonary hypertensive rats. Environ Res 95, 71-76.

Lui, K.H., Bandowe, B.A., Ho, S.S., Chuang, H.C., Cao, J.J., Chuang, K.J., Lee, S.C., Hu, D., Ho, K.F., 2016. Characterization of chemical components and bioreactivity of fine particulate matter (PM2.5) during incense burning. Environ Pollut 213, 524-532.

M., D.A., J., S.J., Yuanhang, Z., Limin, Z., R., C.G., 2006. Size□resolved particulate matter composition in Beijing during pollution and dust events. J Geophys Res Atmos 111.

435 Ma, Y., Zhang, H., Zhao, Y., Zhou, J., Yang, S., Zheng, X., Wang, S., 2017. Short-term effects of air
436 pollution on daily hospital admissions for cardiovascular diseases in western China. Environ Sci Pollut
437 Res Int 24, 14071-14079.
438 Meng, Z., Zhang, Q., 2007. Damage effects of dust storm PM2.5 on DNA in alveolar macrophages and
439 lung cells of rats. Food Chem Toxicol 45, 1368-1374.
440 Naimabadi, A., Ghadiri, A., Idani, E., Babaei, A.A., Alavi, N., Shirmardi, M., Khodadadi, A., Marzouni,
441 M.B., Ankali, K.A., Rouhizadeh, A., Goudarzi, G., 2016. Chemical composition of PM10 and its in
442 vitro toxicological impacts on lung cells during the Middle Eastern Dust (MED) storms in Ahvaz, Iran.
443 Environ Pollut 211, 316-324.
444 Paatero, P., 1997. Least squares formulation of robust non-negative factor analysis. Chemometrics and
445 Intelligent Laboratory Systems 37, 23-35.
446 Paatero, P., Tapper, U., 1994. Positive matrix factorization - a nonnegative factor model with optimal
447 utilization of error-estimates of data values. Environmetrics 5, 111-126.
448 Shen, Z.X., Cao, J.J., Arimoto, R., Han, Y.M., Zhu, C.S., Tian, J., Liu, S.X., 2010. Chemical
449 Characteristics of Fine Particles (PM1) from Xi'an, China. Aerosol Science and Technology 44, 461-
450 472.
451 Shen, Z.X., Cao, J.J., Arimoto, R., Han, Z.W., Zhang, R.J., Han, Y.M., Liu, S.X., Okuda, T., Nakao, S.,
452 Tanaka, S., 2009. Ionic composition of TSP and PM2.5 during dust storms and air pollution episodes at
453 Xi'an, China. Atmospheric Environment 43, 2911-2918.
454 Sun, J., Zhang, M., Liu, T., 2001. Spatial and temporal characteristics of dust storms in China and its
455 surrounding regions, 1960–1999: Relations to source area and climate. J Geophys Res Solid Earth
456 Atmospheres 106, 10325-10333.
457 Ta, W.Q., Xiao, Z., Qu, J.J., Yang, G.S., Wang, T., 2003. Characteristics of dust particles from the
458 desert/Gobi area of northwestern China during dust-storm periods. Environmental Geology 43, 667-679.
459 Tam, W.W., Wong, T.W., Wong, A.H., 2012. Effect of dust storm events on daily emergency
460 admissions for cardiovascular diseases. Circ J 76, 655-660.
461 Teng, J.C., Chan, Y.S., Peng, Y.I., Liu, T.C., 2016. Influence of Asian dust storms on daily acute
462 myocardial infarction hospital admissions. Public Health Nurs 33, 118-128.
463 Vichai, V., Kirtikara, K., 2006. Sulforhodamine B colorimetric assay for cytotoxicity screening. Nat
464 Protoc 1, 1112-1116.

Wang, P., Cao, J.J., Shen, Z.X., Han, Y.M., Lee, S.C., Huang, Y., Zhu, C.S., Wang, Q.Y., Xu, H.M., Huang, R.J., 2015. Spatial and seasonal variations of PM2.5 mass and species during 2010 in Xi'an, China. Science of the Total Environment 508, 477-487.

Wang, X., Dong, Z., Yan, P., Yang, Z., Hu, Z., 2005. Surface sample collection and dust source analysis in northwestern China. CATENA 59, 35-53.

Watanabe, M., Kurai, J., Sano, H., Yamasaki, A., Shimizu, E., 2015. Difference in Pro-Inflammatory Cytokine Responses Induced in THP1 Cells by Particulate Matter Collected on Days with and without ASIAN Dust Storms. Int J Environ Res Public Health 12, 7725-7737.

Watanabe, M., Yamasaki, A., Burioka, N., Kurai, J., Yoneda, K., Yoshida, A., Igishi, T., Fukuoka, Y., Nakamoto, M., Takeuchi, H., Suyama, H., Tatsukawa, T., Chikumi, H., Matsumoto, S., Sako, T., Hasegawa, Y., Okazaki, R., Horasaki, K., Shimizu, E., 2011. Correlation between Asian dust storms and worsening asthma in Western Japan. Allergol Int 60, 267-275.

Wu, F., Chow, J.C., An, Z., Watson, J.G., Cao, J., 2011a. Size-differentiated chemical characteristics of Asian paleo dust: records from aeolian deposition on Chinese Loess Plateau. J Air Waste Manag Assoc 61, 180-189.

Wu, F., Chow, J.C., An, Z.S., Watson, J.G., Cao, J.J., 2011b. Size-Differentiated Chemical Characteristics of Asian Paleo Dust: Records from Aeolian Deposition on Chinese Loess Plateau. Journal of the Air & Waste Management Association 61, 180-189.

Wu, F., Zhang, D.Z., Cao, J.J., Guo, X., Xia, Y., Zhang, T., Lu, H., Cheng, Y., 2017. Limited production of sulfate and nitrate on front-associated dust storm particles moving from desert to distant populated areas in northwestern China. . Atmos. Chem. Phys. 17, 14473-14484.

Xu, H.M., Cao, J.J., Ho, K.F., Ding, H., Han, Y.M., Wang, G.H., Chow, J.C., Watson, J.G., Khol, S.D., Qiang, J., Li, W.T., 2012. Lead concentrations in fine particulate matter after the phasing out of leaded gasoline in Xi'an, China. Atmospheric Environment 46, 217-224.

Zaady, E., Offer, Z.Y., Shachak, M., 2001. The content and contributions of deposited aeolian organic matter in a dry land ecosystem of the Negev Desert, Israel. Atmos Environ 35, 769-776.

Zhang, B., Tsunekawa, A., Tsubo, M., 2008. Contributions of sandy lands and stony deserts to long-distance dust emission in China and Mongolia during 2000–2006. Glob Planet Change 60, 487-504.

Zhang, R., Cao, J., Tang, Y., Arimoto, R., Shen, Z., Wu, F., Han, Y., Wang, G., Zhang, J., Li, G., 2014. Elemental profiles and signatures of fugitive dusts from Chinese deserts. Sci Total Environ 472, 1121-1129.

496 Zhang, R., Jing, J., Tao, J., Hsu, S.C., Wang, G., Cao, J., Lee, C.S.L., Zhu, L., Chen, Z., Zhao, Y., Shen,
497 Z., 2013. Chemical characterization and source apportionment of PM2.5 in Beijing: seasonal
498 perspective. Atmospheric Chemistry and Physics 13, 7053-7074.
499 Zhang, T., Cao, J.J., Tie, X.X., Shen, Z.X., Liu, S.X., Ding, H., Han, Y.M., Wang, G.H., Ho, K.F.,
500 Qiang, J., Li, W.T., 2011. Water-soluble ions in atmospheric aerosols measured in Xi'an, China:
501 Seasonal variations and sources. Atmospheric Research 102, 110-119.
502 Zosky, G.R., Boylen, C.E., Wong, R.S., Smirk, M.N., Gutierrez, L., Woodward, R.C., Siah, W.S.,
503 Devine, B., Maley, F., Cook, A., 2014. Variability and consistency in lung inflammatory responses to
504 particles with a geogenic origin. Respirology 19, 58-66.

505

506 **Table 1. Average (± SD) mass concentration (μg·m^{-3}) and chemical composition contributions to particulate matter of <2.5 μm**
507 **in aerodynamic diameter ($PM_{2.5}$; %) in Xi'an and Beijing**

Chemical Species	Xi'an Normal	Xi'an PE	Xi'an DS-1	Xi'an DS-2	Beijing Normal	Beijing PE	Beijing DS-1	Beijing DS-2
$PM_{2.5}$	96.7±33.6	221.2±59.8	66.8±15.7	82.9±6.1	79.6±38.9	175.9±64.4	49.3±15.2	115.1±20.9
OC	12.3±2.9	12.0±0.2	16.5±3.9	15.9±2	18.0±5.4	14.2±2.7	16.9±2.9	14.0±1.7
EC	4.4±1.1	5.3±0.5	6.3±1.5	7.0±1.3	4.8±1.6	4.9±0.2	4.8±1.2	4.1±0.0
Cl^-	1.2±0.3	1.5±0.5	1.1±0.1	1.1±0.5	3.9±1.3	4.3±0.7	5.1±0.9	2.6±0.5
NO_3^-	21.0±3.9	25.9±5.4	19.7±4.9	15.3±0.7	20.1±8	23.9±4.6	6.8±8.1	6.7±5.8
SO_4^{2-}	17.0±4.2	11.4±2.1	13.3±2.1	14.3±3.8	14.4±4.3	13.7±3.9	11.1±2.2	7.9±1.6
NH_4^+	7.7±2.8	7.8±2.2	3.5±2.4	4.9±1.4	3.3±3.0	7.4±2.5	0.1±0.0	1.4±1.4
K^+	1.3±0.3	1.5±0.3	1.1±0.1	1.3±0.1	1.1±0.4	1.6±0.3	1.3±0.6	0.7±0.4
Mg^{2+}	0.3±0.1	0.2±0.1	0.5±0.1	0.3±0.0	0.7±0.3	0.4±0.1	1.5±0.4	0.5±0.0
Ca^{2+}	1.5±1.3	1.9±0.1	1.9±0.3	0.8±0.3	6.8±2.9	3.4±1.0	11.3±1.8	3.6±0.9
S	3.31±0.66	2.32±0.06	3.03±0.50	2.9±0.62	2.02±0.54	2.37±0.34	1.27±0.26	1.30±0.55
Ca	0.37±0.29	0.83±0.38	1.08±0.25	1.02±0.27	2.68±1.24	1.68±0.92	5.83±2.19	2.56±0.40
Ti	0.03±0.02	0.04±0.01	0.05±0.02	0.07±0.01	0.06±0.05	0.06±0.04	0.27±0.17	0.27±0.05
Mn	0.004±0.002	0.002±0.002	0.008±0.003	0.007±0.000	0.006±0.004	0.003±0.000	0.010±0.004	0.012±0.006
Fe	0.03±0.01	0.03±0.00	0.04±0.01	0.05±0.00	0.05±0.02	0.05±0.01	0.13±0.03	0.09±0.01
Zn	0.52±0.21	0.61±0.16	0.89±0.16	1.00±0.15	1.18±0.5	1.06±0.48	3.59±1.47	2.90±0.39
Pb	0.38±0.44	0.15±0.02	0.18±0.13	0.66±0.10	0.15±0.06	0.21±0.04	0.15±0.13	0.18±0.10
V	0.10±0.04	0.08±0.01	0.08±0.06	0.11±0.01	0.13±0.04	0.1±0.04	0.13±0.06	0.08±0.01

508 PE, pollution episode; DS, dust storm period; OC, organic carbon; EC, elemental carbon.

509

510

Table 2. Correlations of the bioreactivity (cell viability and cytotoxicity-related lactate dehydrogenase (LDH)) with particulate matter of <2.5 μm in aerodynamic diameter ($PM_{2.5}$) and PMF-sourced $PM_{2.5}$ from biomass, coal, industrial, vehicle, secondary inorganic aerosol (SNA), and dust storm (dust) emissions during the entire study period (All), normal days (Normal), and dust storms (Dust) in Xi'an and Beijing

	Xi'an						Beijing					
	All		Normal		Dust		All		Normal		Dust	
	Cell viability	LDH	Cell viability	LDH	Cell viability	LDH	Cell viability	LDH	Cell viability	LDH	Cell viability	LDH
$PM_{2.5}$	-0.305	0.100	**-0.463***	0.237	0.500	-0.540	0.044	0.269	-0.033	0.441	-0.187	**0.938***
$PM_{2.5}$ emission sources												
Biomass	-0.229	0.261	-0.268	0.257	**-0.922***	**0.930***	-0.272	0.139	-0.124	0.065	-0.771	-0.307
Coal	-0.004	-0.157	-0.117	-0.110	0.776	-0.782	0.267	-0.252	0.446	-0.302	-0.344	-0.210
Industrial	**-0.693***	**0.663***	**-0.659***	**0.673***	**-0.939***	**0.950***	0.216	-0.007	-0.064	0.437	-0.603	0.465
Vehicle	**-0.567***	**0.419***	**-0.695***	**0.581***	0.123	-0.134	0.194	-0.152	**-0.542***	**0.496***	-0.406	**0.922***
SNA	-0.287	0.084	-0.317	0.180	-0.475	0.437	-0.011	0.209	0.143	0.263	-0.572	0.705
Dust	-0.247	0.326	-0.075	0.179	0.623	-0.660	-0.180	0.374	-0.233	0.219	0.443	0.598

* $p<0.05$

Table 3. Correlations between chemical components in particulate matter of <2.5 μm in aerodynamic diameter ($PM_{2.5}$) and the bioreactivity (cell viability and cytotoxicity-related lactate dehydrogenase (LDH)) for biomass and industrial emissions in Xi'an and vehicle emissions in Beijing during the entire study period (All) and dust storms (Dust)

	Xi'an								Beijing			
	All				Dust				All		Dust	
	Biomass		Industrial		Biomass		Industrial		Vehicle		Vehicle	
	Cell viability	LDH	Cell viability	LDH	Cell viability	LDH	Cell viability	LDH	Cell viability	LDH	Cell viability	LDH
OC	-0.279	**0.484***	**-0.485***	**0.555***	-0.586	0.624	**-0.967***	**0.959***	0.313	-0.326	-0.349	**0.839***
EC	-0.354	**0.527***	**-0.534***	**0.599***	-0.611	0.647	**-0.981***	**0.973***	0.260	-0.265	-0.463	**0.863***
Cl^-	-0.262	0.406	**-0.529***	**0.551***	**-0.845***	**0.864***	**-0.911***	**0.892***	0.232	-0.244	-0.631	0.632
NO^{3-}	-0.143	0.269	**-0.564***	**0.585***	**-0.960***	**0.962***	-0.822	**0.800***	0.207	-0.203	-0.727	0.568
SO_4^{2-}	0.043	0.100	**-0.553***	**0.557***	-0.551	0.587	-0.792	0.788	0.123	-0.064	-0.567	**0.858***
NH_4^+	0.192	-0.214	**-0.651***	**0.610***	-0.359	0.332	-0.732	0.723	0.054	-0.013	-0.581	0.705
K^+	-0.220	0.317	**-0.597***	**0.635***	-0.739	0.764	**-0.894***	**0.885***	0.133	-0.139	-0.723	0.567
Mg^{2+}	-0.263	0.495	**-0.430***	**0.505***	-0.645	0.677	**-0.839***	**0.823***	0.255	-0.257	-0.569	0.609
Ca^{2+}	**-0.519***	**0.592***	-0.336	**0.426***	-0.859	0.876	-0.701	0.670	0.287	-0.338	-0.642	0.475
S	-0.066	0.228	**-0.514***	**0.509***	-0.571	0.605	-0.810	0.802	0.098	-0.067	-0.647	**0.846***
Ca	-0.375	0.551	-0.311	**0.521***	**-0.639***	**0.673***	**-0.967***	**0.956***	0.212	-0.225	-0.386	0.693
Ti	-0.188	0.408	-0.349	**0.562***	-0.482	0.520	**-0.983***	**0.974***	-0.051	0.262	-0.065	**0.949***
V	-0.270	0.253	**-0.465***	**0.409***	-0.539	0.527	-0.807	0.797	0.236	-0.002	0.477	0.649
Mn	-0.238	0.441	**-0.478***	**0.528***	-0.520	0.546	**-0.887***	**0.873***	0.080	0.005	-0.380	**0.815***
Fe	-0.250	0.482	**-0.463***	**0.623***	-0.609	0.643	**-0.974***	**0.963***	0.086	0.043	-0.205	**0.943***
Zn	**0.391***	-0.133	**-0.387***	0.363	-0.122	0.114	**-0.992***	**0.986***	0.121	-0.100	-0.709	0.730
Pb	0.046	0.073	**-0.578***	**0.608***	-0.441	0.443	**-0.871***	**0.851***	0.292	-0.286	-0.567	0.608

OC, organic carbon; EC, elemental carbon.

* $p<0.05$

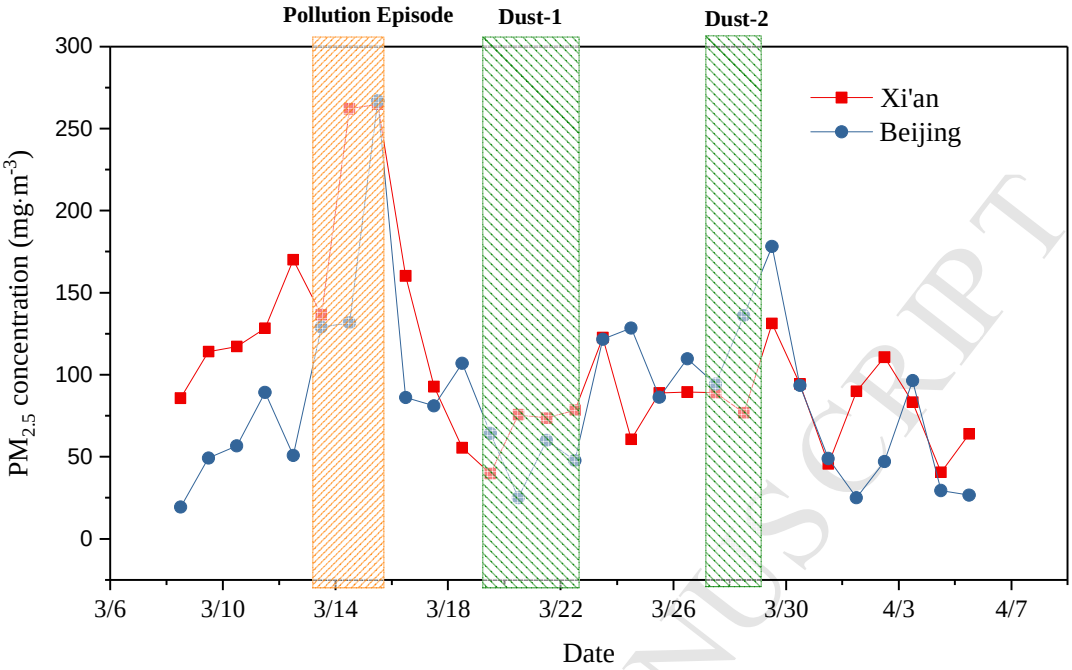

522

523 **Figure 1. Daily variations in particulate matter of <2.5 μm in aerodynamic diameter ($PM_{2.5}$)**
524 **concentrations in Xi'an and Beijing.**

525

526

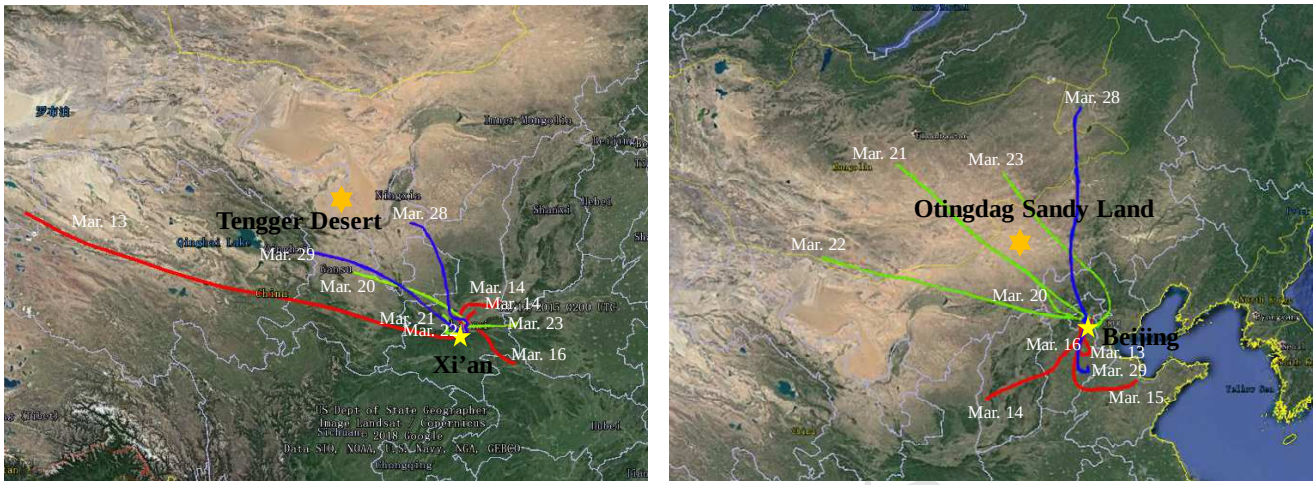

527

528 **Figure 2. Back trajectories for Xi'an and Beijing on polluted days. Red lines, Pollution Episode;**
529 **green lines, Dust-1; blue lines, Dust-2.**

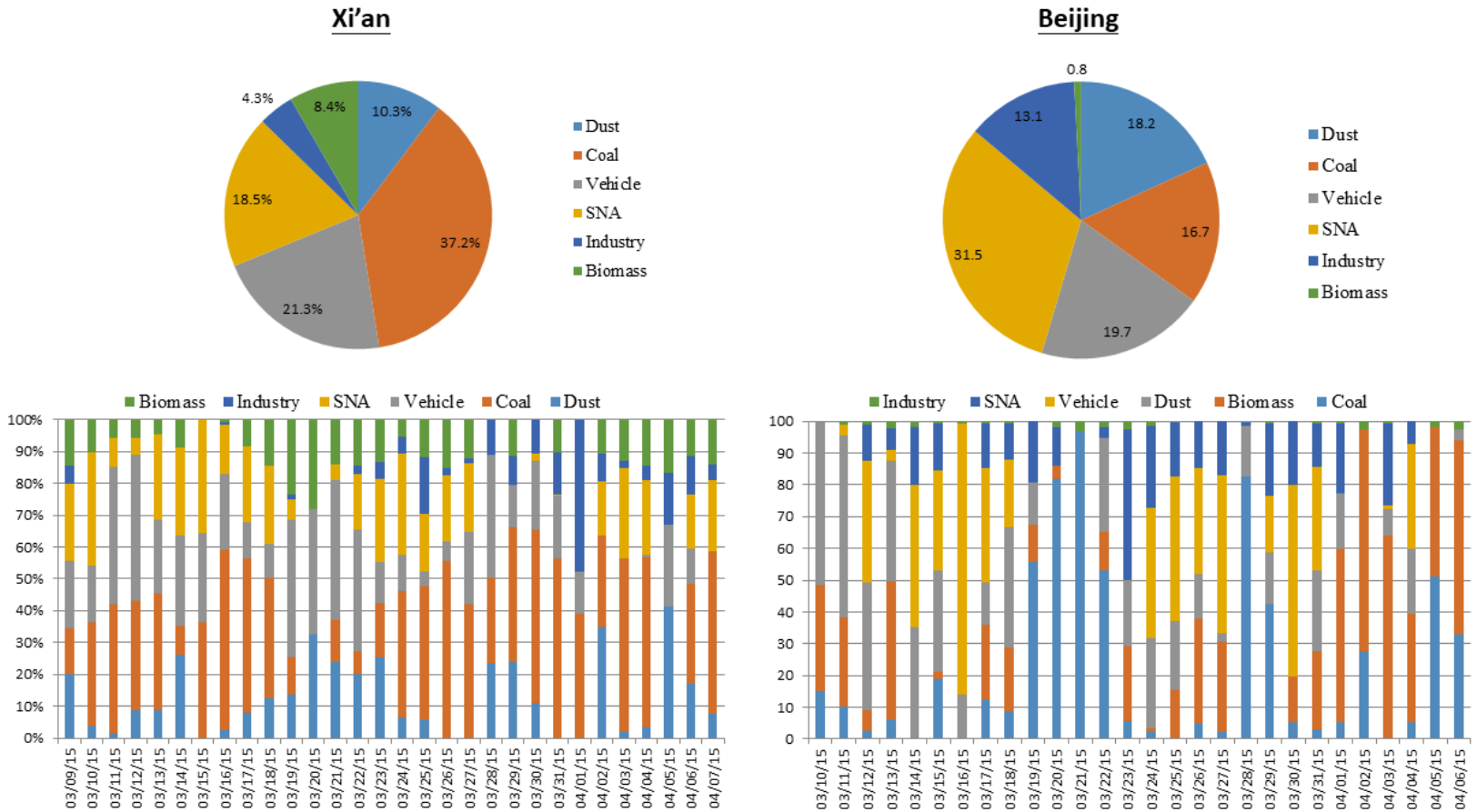

Figure 3. Sources and relative contributions of each source to particulate matter of <2.5 μm in aerodynamic diameter ($PM_{2.5}$) by positive matrix factorization (PMF) during the sampling period in both Xi'an and Beijing.

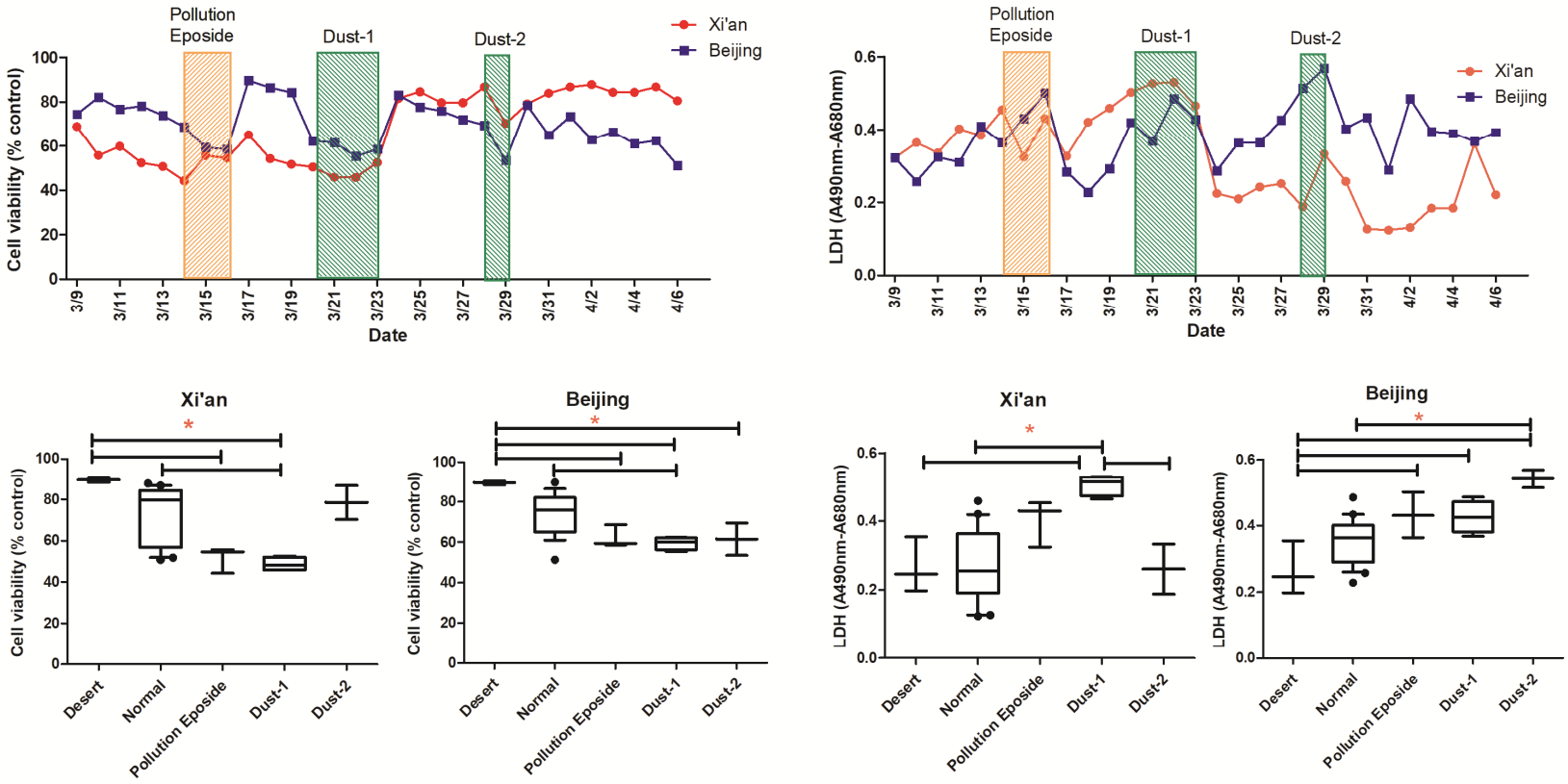

Figure 4. Sequential bioreactivity caused by particulate matter of <2.5 μm in aerodynamic diameter ($PM_{2.5}$) at 50 μg/mL in A549 cells, including cell viability (% control) and cytotoxicity-related lactate dehydrogenase (LDH) during the study periods. The cell viability and LDH caused by $PM_{2.5}$ from the desert, normal days, pollution episode, dust-1 (first dust storm), and dust-2 (second dust storm) in Xi'an and Beijing. * p<0.05.

Highlights

- Contributions of $PM_{2.5}$ emissions to bioreactivity during dust storm were investigated.
- Emissions of from local $PM_{2.5}$ sources caused deterioration of air quality during dust storms.
- Sand dust interacted with chemicals leading to increase of $PM_{2.5}$bioreactivity.

Key words: air pollution, cell viability, inflammation, oxidative stress, wind speed.